### Title

Segregation of four Agrobacterium tumefaciens replicons during polar growth: PopZ and PodJ control segregation of essential replicons




### Journal

Proceedings of the National Academy of Sciences of the United States of America, 117(42)

### ISSN

0027-8424



### Authors

Robalino-Espinosa, JS
Zupan, JR
Chavez-Arroyo, A
et al.



### Publication Date

2020-10-20

### DOI

10.1073/pnas.2014371117

Peer reviewed

# Segregation of four *Agrobacterium tumefaciens* replicons during polar growth: PopZ and PodJ control segregation of essential replicons

J. S. Robalino-Espinosa[a,b], J. R. Zupan[a], A. Chavez-Arroyo[a], and P. Zambryski[a,1]

[a]Department of Plant and Microbial Biology, University of California, Berkeley, CA 94720; and [b]Department of Molecular and Cell Biology, Vrije Universiteit Amsterdam, 1081 HV Amsterdam, The Netherlands

Contributed by Patricia Zambryski, September 2, 2020 (sent for review July 8, 2020; reviewed by Christian Baron and Walter Ream)

***Agrobacterium tumefaciens*** **C58 contains four replicons, circular chromosome (CC), linear chromosome (LC), cryptic plasmid (pAt), and tumor-inducing plasmid (pTi), and grows by polar growth from a single growth pole (GP), while the old cell compartment and its old pole (OP) do not elongate. We monitored the replication and segregation of these four genetic elements during polar growth. The three largest replicons (CC, LC, pAt) reside in the OP compartment prior to replication; post replication one copy migrates to the GP prior to division. CC resides at a fixed location at the OP and replicates first. LC does not stay fixed at the OP once the cell cycle begins and replicates from varied locations 20 min later than CC. pAt localizes similarly to LC prior to replication, but replicates before the LC and after the CC. pTi does not have a fixed location, and post replication it segregates randomly throughout old and new cell compartments, while undergoing one to three rounds of replication during a single cell cycle. Segregation of the CC and LC is dependent on the GP and OP identity factors PopZ and PodJ, respectively. Without PopZ, replicated CC and LC do not efficiently partition, resulting in sibling cells without CC or LC. Without PodJ, the CC and LC exhibit abnormal localization to the GP at the beginning of the cell cycle and replicate from this position. These data reveal PodJ plays an essential role in CC and LC tethering to the OP during early stages of polar growth.**

*Agrobacterium tumefaciens* | polar growth | replication and segregation | multipartite genomes | PopZ and PodJ

Alphaproteobacteria (especially the order Rhizobiales) have complex genomes with multiple elements classified as primary or secondary chromosomes, as well as very large plasmids (1, 2). The 5.67-Mb sequenced genome of the well-known Rhizobiales pathogen, *Agrobacterium tumefaciens* C58, is organized into four replicons, circular chromosome (CC) (2.8 Mbp), secondary linear chromosome (LC) (2.0 Mbp), cryptic plasmid (pAt) (0.5 Mbp), and tumor-inducing plasmid (pTi) (0.2 Mbp) (3, 4). Essential genes are present only on CC and LC (3, 4). Multipartite genomes have arisen independently in nearly 10% of bacterial species from diverse phyla (5). The prevalence of multipartite organization in plant symbionts (*Sinorhizobium meliloti*) (6), plant pathogens (*A. tumefaciens*) (3, 4), animal symbionts (*Vibrio fisheri*) (7), and animal (*Brucella abortus*) (8) and human (*Vibrio cholerae*) (9) pathogens suggests that a divided genome may be important for viability in diverse niches by enabling coordinated expression of sets of genes in response to specific conditions (5). For example, pAt encodes proteins for diverse metabolic and detoxification functions likely advantageous in the species-rich, competitive soil environment (3, 4, 10), and pTi encodes essential functions specific to virulence that create the unique plant tumor environment exploited by *Agrobacterium* (10, 11).

Multipartite genomes, however, likely require mechanisms that coordinate replication and segregation of replicons to ensure sibling cells inherit complete genomes. Each of the four genetic elements in *Agrobacterium* encodes its own segregation system that includes a specific binding site and factors that bind to this site to facilitate separation and partitioning of newly replicated chromosomal elements. The CC encodes a *parABS* partitioning system (2), whereas LC, pTi, and pAt each encode their own *repABC* cassette (2–4).

An early report described two patterns of localization for the four replicons of *Agrobacterium*: CC, LC, and pAt localization was either unipolar in short cells or bipolar in longer cells, while pTi exhibited a subpolar localization pattern in short and long cells (12). These studies were performed before it was known that *Agrobacterium* undergoes polar growth from a single pole (13–15). Polar growth produces two distinct poles, an actively growing new growth pole (GP), and a nongrowing old pole (OP) (Fig. 1). A more recent study focused on the *Agrobacterium* CC (16); CC first localized to the OP, and after replication, one CC remained at the OP, while the other migrated to the GP. After division, each sibling had a CC localized at their OP.

Here we characterize and compare the replication and segregation of all four *Agrobacterium* replicons (CC, LC, pAt, pTi) during polar growth. There are several obvious questions: 1) do all replicons localize to the OP prior to replication, or do some replicons replicate at other locations; 2) where do replicons migrate during their segregation; and 3) what is the timing of replication and segregation of the different elements? Our studies were facilitated by the ability to distinguish the GP and

## Significance

**Bacteria are ubiquitous, essential, and remarkably diverse. Many infectious species do not follow rules established in model bacteria where growth occurs by insertion of new material along the cell length; instead, many pathogens grow from their poles. Pathogenic bacteria also carry multipartite genomes for adaptation to different ecological niches. How multiple chromosomes replicate and segregate in the context of polar growth is largely unknown. Here, four replicons of the plant pathogen *Agrobacterium tumefaciens* exhibit distinct temporal and spatial replication/segregation patterns during the polar growth cycle, and specific proteins, targeted to the nongrowing and new growth poles, regulate replicon transmission. Uncovering the mechanisms underlying polar growth and chromosome segregation will present new opportunities to design strategies to limit bacterial diseases.**

Author contributions: J.S.R.-E., J.R.Z., A.C.-A., and P.Z. designed research; J.S.R.-E., J.R.Z., and A.C.-A. performed research; J.S.R.-E., J.R.Z., and P.Z. analyzed data; and J.S.R.-E., J.R.Z., and P.Z. wrote the paper.

Reviewers: C.B., University of Montreal; and W.R., Oregon State University.

The authors declare no competing interest.



[1]To whom correspondence may be addressed. Email: zambrysk@berkeley.edu.

This article contains supporting information online at https://www.pnas.org/lookup/suppl/doi:10.1073/pnas.2014371117/-/DCSupplemental.

First published October 6, 2020.

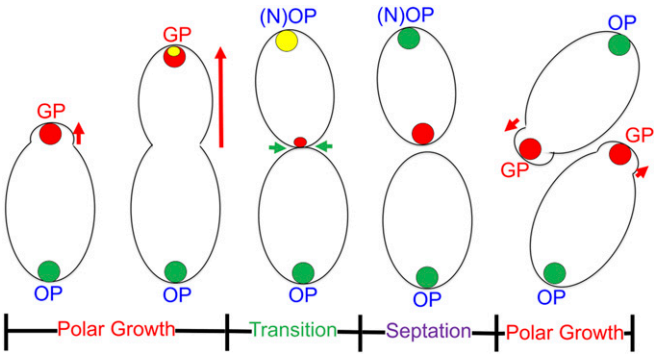


**Fig. 1.** Polar growth in *Agrobacterium*. First, a GP bud is visible in early stages of the cell cycle. PopZ (red circles) is at the GP, and PodJ (green circles) is at the OP. The GP increases in width and length (red arrows), while the OP does not grow. During elongation, PodJ begins to accumulate at the GP (yellow circles, due to colocalization of PopZ and PodJ). When the new cell compartment reaches its final size, the GP transitions into a "new" OP ([N] OP), and the cell divides at the midcell (green arrows) to produce two sibling cells which will restart polar growth. During transition and septation, PopZ is mobilized from the (N)OP to the nascent GP of the upper cell at the septation site. PopZ is synthesized and localized to the new GP in the lower cell as polar growth begins. For details, see refs. 13–18.

OP: the GP has a distinct morphology as a bud with a narrow diameter, while the nongrowing OP has dimensions of a fully grown cell (Fig. 1). Furthermore, GP and OP specific marker proteins have been identified: PopZ marks the GP, and PodJ marks the OP (Fig. 1) (17–19). We demonstrate that each of the four genetic elements exhibits a distinct pattern of localization and timing for their replication and segregation during polar growth. We monitor the replication/segregation of the essential CC and LC in detail and demonstrate that their segregation is critically dependent on PopZ and PodJ.

## Results

We monitored the replication and segregation of the four genetic elements in *A. tumefaciens* strain C58 by fluorescence microscopy of enhanced green fluorescent protein (eGFP) or red fluorescent protein (RFP) fused to the cognate partitioning protein of each genetic element: ParB, CC; RepB, LC; RepB-At, pAt; RepB-Ti, pTi.

**Replication and Segregation of the Agrobacterium Circular Chromosome.** The CC displays a very specific pattern of dynamic localization and movement during polar growth (monitored by eGFP fused to ParB). Immediately after cell division, a sibling cell has already replicated its CC, so that one CC is at the OP, and the other CC has migrated almost halfway through the old cell compartment (Fig. 2*A*, 0′ and Movie S1). In just 10 min, the newly replicated CC arrives at the GP in the new cell compartment. As polar growth continues, the CC remains associated with the GP and ensures one CC copy is segregated to the GP before elongation is complete. The tight association of replicated CC with the GP and OP suggests a mechanism(s) that targets the CC to these specific cellular locations.

While the overall pattern of replication and segregation is similar in sibling cells, the timing of these events is different during late stages of cell elongation when CCs are localized to both the GP and OP (Fig. 2*B* and Movie S2); the shorter, narrower GP compartment (Fig. 2*B*, 0′) is distinguished from the longer nongrowing OP compartment. Just before cell division, the CC in the OP compartment (cell 2) replicates at 40 min. CC replication in the GP compartment sibling (cell 1) occurs at 60 min. Thus, siblings do not replicate their CCs synchronously, as also previously reported (16).

At the population level, the CC mainly localizes as two foci (79%), while 14% of cells contained one focus at the OP, and 7% of cells displayed three foci (Fig. 2*C*). To estimate the timing of CC movement post replication, we plotted the distance of CC (eGFP-ParB foci) from the nongrowing OP versus cell length (Fig. 2*D*). Cell length is an estimate of cell cycle stage during polar growth (20). Foci on the *x* axis or along the diagonal are at OPs or GPs, respectively; foci between these two lines represent foci in transit from the OP to the GP (*SI Appendix*, Fig. S1). The data reveal three trends. First, the shortest cells (1.8–2 μm) have one unreplicated CC at the OP as expected. Many short cells also contain two foci, indicating that CC replication occurs immediately after cell division. Second, in cells with two foci, 66% show newly replicated CCs at the GP, underscoring that CC transit to the GP is rapid; fewer cells (34%) show foci in transit between the *x* axis and the diagonal. Extremely long cells (3.8–4.8 μm) have three foci with CCs localized at the OP, GP, and a third focus just distal to the OP. Cells with three foci support that replication can occur prior to cell division as seen in Fig. 2*B*. Finally, CCs localize to GP in all cells 3 μm and longer; thus, replication and segregation of CC are complete before most new cells are halfway to their final length (~4 μm). As the *A. tumefaciens* cell cycle is ~90 min (in Luria broth [LB] at 28 °C), the CC is replicated and segregated within the first 45 min of the cell cycle. The precision of CC replication/segregation is distinct from that observed for other *Agrobacterium* replicons.

**Replication and Segregation of the Linear Chromosome.** Replication and segregation of the LC (monitored by eGFP-RepB fluorescence) is strikingly complex. In two sibling cells just undergoing cell division, LC foci are at or close to the OP (Fig. 3*A*, 0′ and Movie S3). By 30′, the single LC focus in sibling cell 2 migrates through the old cell compartment and localizes just below the junction between the new and old cell compartments; by 40 min, this LC has replicated, and one copy localizes at the GP, while the other copy moves back to the OP (Fig. 3*A*, 60′, 80′). Like the CC, LC replication is not synchronous in the two siblings, but occurs 20 min later in the younger sibling 1 (Fig. 3*A*, 60′). By 80 min, both siblings have a similar localization of LC at their GPs and OPs. In summary, the LC initially localizes at or near the OP, but, unlike the CC, the LC migrates away from the OP before it replicates. After replication, one LC returns to the OP, while the other copy migrates to the GP.

The frequency of cells with one, two, or more LC foci (Fig. 3*B*) is unlike that observed for the CC (Fig. 2*C*). The LC localizes as two foci at a lower frequency (29.6%) compared to the CC (79%), while more cells contained one focus (50.4%) compared to the CC (14%). The LC also localizes as three (4.8%) or four (1.6%) foci. Unexpectedly, no foci were observed in 13.6% of cells that show a diffuse signal (Fig. 3*B*). Time-lapse imaging shows distinct LC foci can change to a diffuse signal and then return to a distinct focus during the course of a cell cycle (*SI Appendix*, Fig. S2).

To estimate the timing of LC segregation post replication, we plotted the distance of LC foci from the OP (Fig. 3*C*). The distribution of LC foci is clearly different from the CC (Fig. 2*D*). Notably, single LC foci (prior to replication) are widely distributed throughout the entire old cell compartment ranging from the OP in the shortest cells (1.73 μm) to close to the midcell in long cells (3.4 μm). This distribution likely reflects the variable movement of LC foci away from the OP prior to replication as seen by time-lapse microscopy (Fig. 3*A*). Most replicated foci (85%) reside between the poles. Interestingly, some LC foci (15%) localize just below, but not "on" the diagonal as seen for CC; thus, the LC is slightly distal to the GP post segregation. Cells with three LC foci occur in cells as short as 2.5 μm

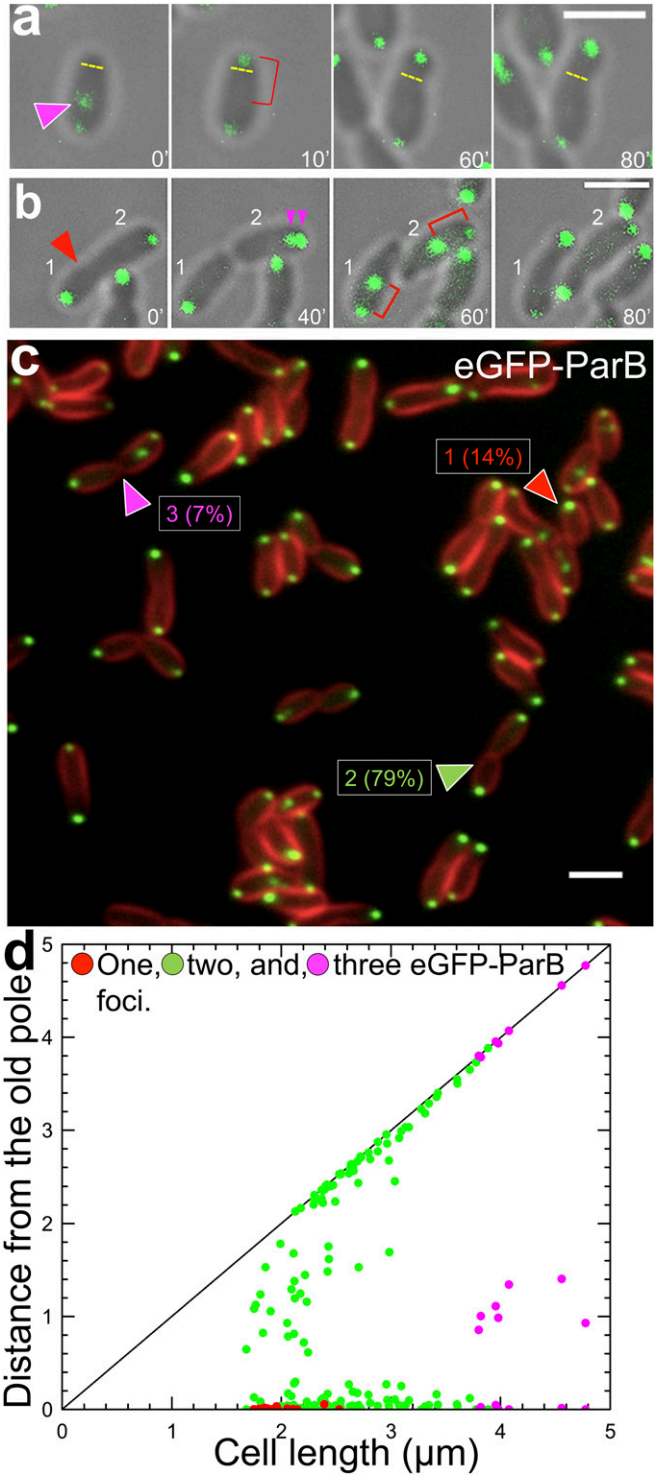


**Fig. 2.** Replication and segregation of the CC during polar growth. (*A*) Time-lapse imaging of CC localization (monitored as eGFP-ParB fluorescence). Yellow dashed line indicates the boundary between the older sibling and the emerging newer sibling. The CC is already replicated at 0′ (magenta arrowhead). CC migration to GP (red bracket) is complete by 10′ where it remains during polar growth (up to 80′ shown). (*B*) Time lapse of asynchronous CC replication in sibling cells 1 and 2. CCs are at the GP (nascent sibling 1, red arrowhead), and at the OP in nascent sibling 2 (0′). The CC replicates in nascent sibling 2 (40′, double magenta arrowheads) but not in the still elongating nascent sibling 1. The CC in sibling 1 replicates between 40′ and 60′. Migration of both newly replicated CC (60′, red brackets) to new GPs is complete by 80′. (*C*) Localization of eGFP-ParB in 100 FM4-64 stained cells. Percentages of cells displaying one, two, or three foci, are shown with, red, green, and magenta arrowheads. (*D*) Distances of eGFP-ParB foci from the OP in 100 cells containing one (red), two (green), or three (magenta) foci are plotted versus cell length. Foci on the *x* axis are at the OP, and foci on the diagonal are at the GP. Foci between the *x* axis and the diagonal represent foci in transit to the GP; 27 such foci can be easily seen, representing 34% of cells with two foci (i.e., 27 out of 79 cells with two foci); by corollary, 66% of cells have their newly replicated CC at the GP. (Scale bars in *A*–*C*, 2 μm.)

suggesting that occasionally (4.8%) there may be a second round of LC replication during the elongation phase of the cell cycle. Four LC foci occur in elongating cells with an average length of 3.75 μm, less than the 4 μm achieved just prior to cell division. Thus, the LC displays variable localization and replication patterns.

**The Circular Chromosome Replicates First and Arrives at the Growth Pole before the Linear Chromosome.** To determine the timing of CC versus LC replication/segregation we coexpressed eGFP-ParB (binds to CC) and RFP-RepB (binds to LC) and monitored their dynamics (Fig. 4 and Movie S4). At 0 min, the CC has replicated, revealing one CC at the OP and one CC in the middle of the old cell compartment; at this time, the LC localizes just above the OP. At 10 min, the newly replicated CC arrives in the new cell compartment, while the LC has not moved. By 20 min, the newly replicated CC arrives at the GP, and the LC has just replicated. At 30 min, CC localization has not changed, while the newly replicated LC arrives in the new cell compartment. The LC arrives at the GP at 40 min. In summary, the LC replicates 20 min later than the CC and arrives at the GP 20 min later than the CC.

**Replication and Segregation of the Cryptic Plasmid.** Replication and segregation of the cryptic At plasmid was monitored by eGFP-RepB-At (Fig. 5 and Movie S5). Just after cell division, sibling cells inherit a single pAt at their OPs (Fig. 5*A*, 0′). Similar to the LC, pAt first migrates away from the OP. The distance migrated prior to replication varies between siblings; in sibling 1, pAt migrates to more than midway through the old cell compartment, while in sibling 2, pAt migrates a short distance from the OP (Fig. 5*A*, 40′). Sibling 2 replicates pAt at 40′, while sibling 1 replicates pAt at 70′. The newly replicated pAt arrives at the GP at 70′ in sibling 2 and at 90′ in sibling 1. By 90′, both siblings have pAt at their GP and OP.

pAt mainly localizes as single foci (64%), 31% showed two foci, 3% showed diffuse signal, and a few cells showed three (1%) or four (1%) foci (not visible in the field of view in Fig. 5*B*). As above, cells with three or four foci suggest a second round of replication occurs before the cell cycle ends (see also *SI Appendix*, Fig. S3). There is a wide distribution of single pAt foci prior to replication, ranging from foci at the OP in the shortest cells to foci near the middle of the old cell compartment (ranging in size from 1.49~2.64 μm in length) (Fig. 5*C*), but not as great a range as displayed by the LC (Fig. 3*C*). Cells with two foci resemble the CC in their distribution with most foci at (or very close to) the GP (81%) and few cells in transit to the GP (19%). However, upon arrival in the new cell compartment, pAt requires 30 min to arrive at the GP (Fig. 5*D*), while the CC is at the GP immediately upon arrival in the new cell compartment and stays at the GP during polar growth (Fig. 2*A*).

Due to their variable localization prior to replication, it is difficult to deduce the order of LC versus pAt replication from plots of cell lengths during the entire cell cycle (Figs. 3*C* and 5*C*). To precisely determine the order of LC versus pAT replication, we measured the lengths of only the very shortest cells with two foci for each replicon. *SI Appendix*, Table S1 shows the mean cell

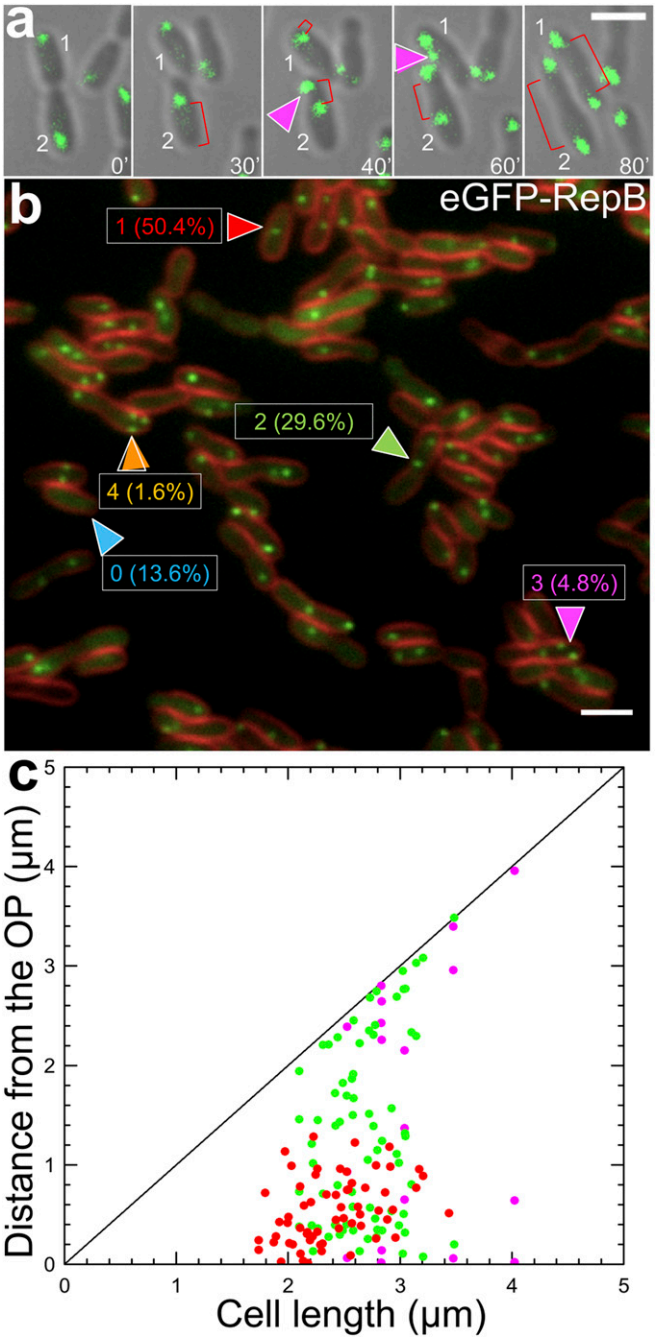


**Fig. 3.** Replication and segregation of the LC during polar growth. (*A*) Time lapse of LC localization (monitored as eGFP-RepB fluorescence). At 0′, two siblings (1, 2) have an LC very near their OP. By 30′, the LC in the lower older (slightly longer) cell (cell 2) has migrated (red bracket) to the junction between the new and old cell compartments, while LC in the upper cell (cell 1) remains at its OP. At 40′ a newly replicated LC (cell 2, magenta arrowhead) has moved (red bracket) close to the GP, while its other copy remains in the old cell compartment. At 40′ the LC in cell 1 has moved away from the old pole (red bracket). Replication of the LC in cell 1 does not initiate until 60′ (cell 1, magenta arrowhead), while one LC copy in cell 2 is migrating (red bracket) back toward the OP. By 80′, one LC is at the GP, and the other LC has migrated back to the OP in both cells 1 and 2 (red brackets). (*B*) Localization of eGFP-RepB in 125 FM4-64 stained cells. Percentages of cell displaying one, two, three, or four foci are shown with red, green, magenta, or orange arrowheads; cell with diffuse signal indicated by cyan arrowhead. (*C*) Distance of eGFP-RepB foci from the OP in 100 cells containing one (red), two (green), or three (magenta) foci. (Scale bars in *A* and *B*, 2 μm.)

length for the first observable replication of CC, LC, and pAt is 2.06, 2.61, and 2.4 μm, respectively. Thus, pAt replicates in shorter cells before LC.

**Replication and Segregation of the Ti Plasmid.** Overall, the Ti plasmid (monitored by eGFP- RepB-Ti) does not occupy specific regions of the cell during its replication and segregation (Fig. 6). Cells showed single (33%), two (21%), three (16%), four (8%), five (7%), six (1%), or no (13%) foci. Unexpectedly, the foci are spread throughout the entire distance between the OP and GP with no apparent clustering close to either pole. That single foci localize throughout the old and new cell compartments illustrates that Ti plasmid replication and segregation is independent of cell length and cycle progression during vegetative growth.

**PopZ Is Required for Segregation of Circular and Linear Chromosomes.** Of the four genetic elements in *Agrobacterium*, only CC and LC are required for viability. We were curious whether pole-specific essential factors such as PopZ and PodJ (17–19) are required to ensure partitioning of the essential CC or LC. Loss of PopZ or PodJ strongly impacts polar growth, resulting in ectopic poles, and interrupted cell division (16–18, 21). To remove PopZ, we used a strain carrying a theophylline-binding riboswitch sequence (RS) upstream of the *popZ* open reading frame (ORF) (17). In the presence of theophylline to induce PopZ expression, localization of ParB foci resembled the wild type (WT) (*SI Appendix*, Fig. S4*A* versus Fig. 2*B*). Without theophylline, most cells (74%) exhibit diffuse eGFP-ParB fluorescence (Fig. 7*A*); likely, eGFP-ParB cannot bind to the CC (to produce a focus) because the CC is lost. Indeed, DAPI staining is weak/absent in Δ*popZ* (16, 21). Other PopZ-depleted cells (26%) displayed abnormal morphology, ectopic growth poles, and/or multiple foci at abnormal locations (Fig. 7*A*).

Cells without a ParB focus previously were observed in only 28% of cells carrying a genetic deletion of *popZ* (16). Our strategy to induce PopZ depletion may constitute a more severe and acute loss of PopZ. This difference is underscored by the discovery that genetic deletion of *popZ* frequently produced revertants that grew like WT when purified from single colonies and cultured (17). Thus, *popZ* deletion strains likely exist as a mixed population of mutant and WT cells.

PopZ is also essential for LC partitioning. We expressed eGFP-RepB in the RS-*popZ* strain. With theophylline, cells resembled WT (*SI Appendix*, Fig. S4*B* versus Fig. 3*B*). In contrast, most cells (57%) grown without theophylline show diffuse or no

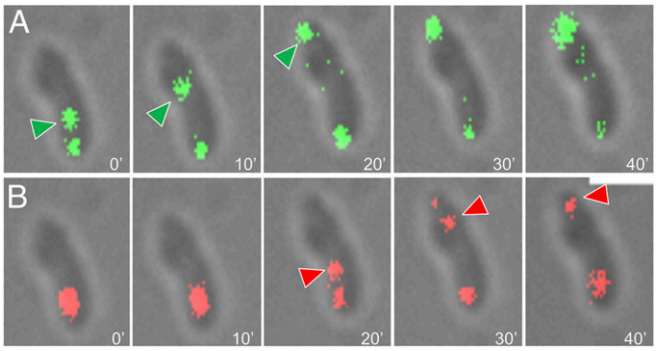


**Fig. 4.** The circular chromosome replicates and arrives at the growth pole before the linear chromosome. Time lapse of the CC and LC chromosomes (monitored by eGFP-ParB [CC] and RFP-RepB [LC] fluorescence, respectively); (*A*) CC and (*B*) LC. Green and red arrowheads indicate newly replicated CC and LC chromosomes, respectively, and show their movement to the GP. (Scale bar, 2 μm.)

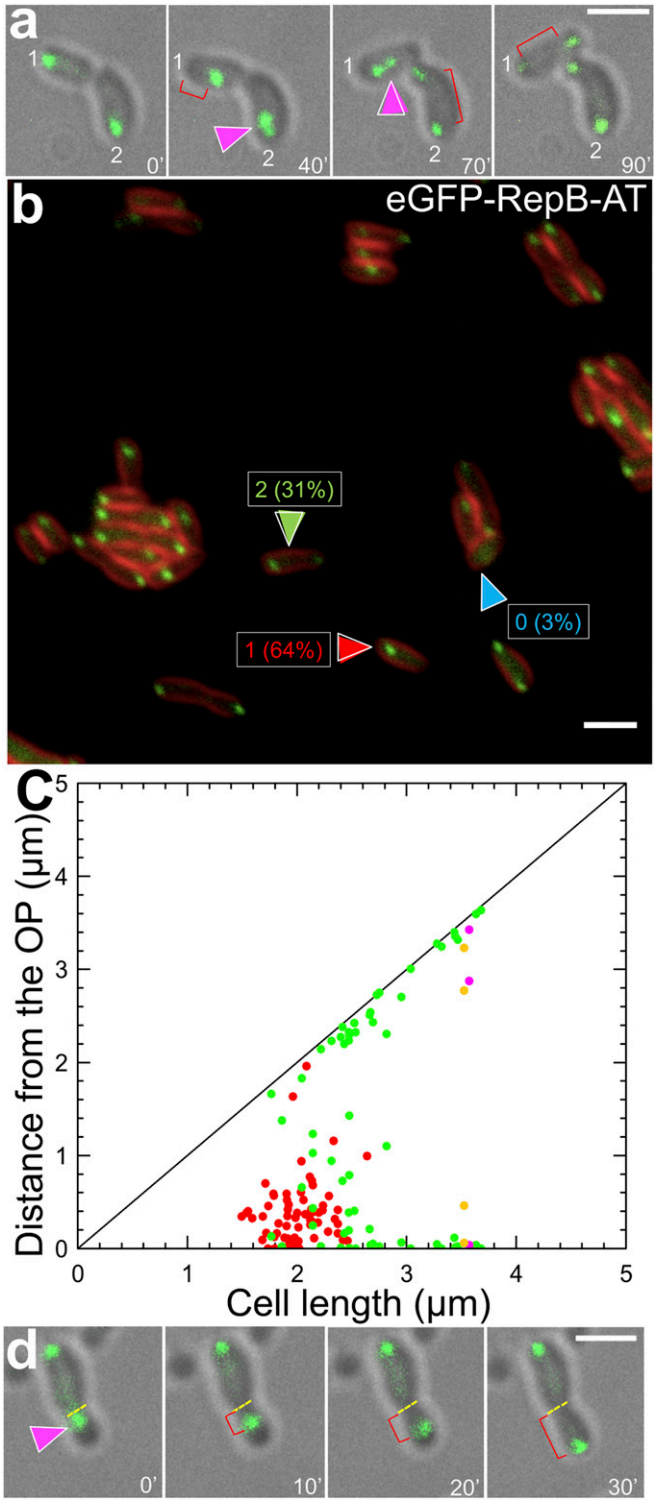


**Fig. 5.** Replication and segregation of the pAt during polar growth. (*A*) Time-lapse imaging of eGFP-RepB-At. At 0′, two sibling cells inherit a single focus of eGFP-RepB-At at each OP. At 40′, pAt has replicated (magenta arrowhead) in cell 2, and pAt in cell 1 migrates toward the midcell (red bracket). At 70′, newly replicated pAt in cell 2 moves (red bracket) toward the GP, and pAt in cell 1 replicates (magenta arrowhead). By 90′, newly replicated pAt in cell 1 moves (red bracket) to the GP. (*B*) Localization of eGFP-RepB-At in 100 FM4-64 stained cells. Percentages of cell displaying one or two foci are shown in red or green, and cells with a diffuse signal are indicated in cyan. (*C*) Distance of eGFP-RepB-At foci from the OP in 100 cells containing one (red), two (green), three (magenta), or four (orange) foci. (*D*) Timing of pAt arrival at the GP. At 0′ a cell displays two pAt foci, one at the OP and the second copy just inside the new cell compartment (magenta arrowhead; yellow dashed line indicates the boundary between old and new cells). By 10′, this second focus has migrated to the middle of the new cell compartment. At 20′ this focus still has not arrived at the GP. The replicated pAt arrives at the GP at 30′. Red brackets indicate the migration of the replicated pAt. (Scale bars in *A*, *B*, and *D*, 2 μm.)

RepB foci (Fig. 7*B*). Other PopZ-depleted cells (44%) exhibited many foci and abnormal morphology (Fig. 7*B*).

**PodJ Is Required for Old Pole Localization of Circular and Linear Chromosomes.** PodJ identifies the old pole (19), and PodJ is required for the transition of the GP into an OP (18). To determine whether PodJ has a role in CC partitioning, we monitored eGFP-ParB localization in cells carrying a deletion of the ORF of *podJ* (Δ*podJ*) (18). To differentiate between WT and Δ*podJ* strains, we refer to the OP in WT, and the cognate pole lacking PodJ protein in Δ*podJ* as the nongrowth pole (NGP). The CC exhibits remarkably abnormal behavior in Δ*podJ* cells, where the CC no longer localizes to the NGP but instead localizes to the GP at the beginning of the cell cycle (Fig. 8 *A* and *B*, 0′). We monitored 40 movies of individual cells for at least 2 h and observed two main patterns at approximately equal frequency. 1) Following cell division, CC replication continues from the GP used in the previous cell cycle (Fig. 8*A*, 0′, 10′, and Fig. 8*B*, 0′, 10′ 20′, and 120′–170′). 2) Or, following division, a CC moves away from the former GP (Fig. 8*A*, 40′ red bracket) and takes up a position in the middle of the resulting sibling cell post cell division (similar to the location in the other sibling); in both siblings, CC then replicates from this middle location, and one copy migrates to the new GPs resulting from septation (Fig. 8*A*, 50′–70′). The cell in Fig. 8*A* transitions from growing and replicating the CC at the GP in the first cell cycle (0′–30′; only the later stages of this cell cycle are captured) to produce siblings where growth occurs normally from new GPs created at the septum. Nevertheless, these latter cells are abnormal as the CC does not localize to the NGP, but instead localizes to the middle of what was the old cell NGP compartment in the previous division. In contrast, the cell in Fig. 8*B* continues to produce two distinct siblings post cell division (Fig. 8*B*, 120′–170′); one sibling continues to use the previous GP for new growth and CC replication, and the other sibling replicates its CC from the middle of the NGP compartment like the siblings in Fig. 8*A*.

PodJ is also essential for the correct localization and segregation of the LC. In WT, the LC does not have dominant localization patterns prior to and post replication (Fig. 3*C*), making it potentially difficult to assign LC localization in Δ*PodJ*. To facilitate these studies, we used the localization of CC foci to the GP in Δ*podJ* to mark the GP in cells coexpressing CC-eGFP-ParB and LC-RFP-RepB. Surprisingly, in Δ*podJ*, the LC consistently colocalizes with the CC. *SI Appendix*, Fig. S5 presents a gallery of 60 Δ*podJ* cells coexpressing eGFP-ParB and RFP-RepB; 90% of the cells showed yellow fluorescent foci, representing colocalization of CC and LC. Only five cells (*SI Appendix*, Fig. S5, cells numbered 7, 25, 37, 51, and 60) show green and red foci next to each other. As foci are dynamic it is not surprising that they sometimes do not exactly coincide, Fig. 9 shows representative higher-resolution images of three Δ*podJ* cells showing colocalization, or one cell showing both no colocalization and overlapping red and green foci of eGFP-ParB and RFP-RepB. Overall, CC and LC are clearly colocalized or in close proximity. Thus, the LC follows the abnormal pattern of localization of CC in Δ*podJ* cells.

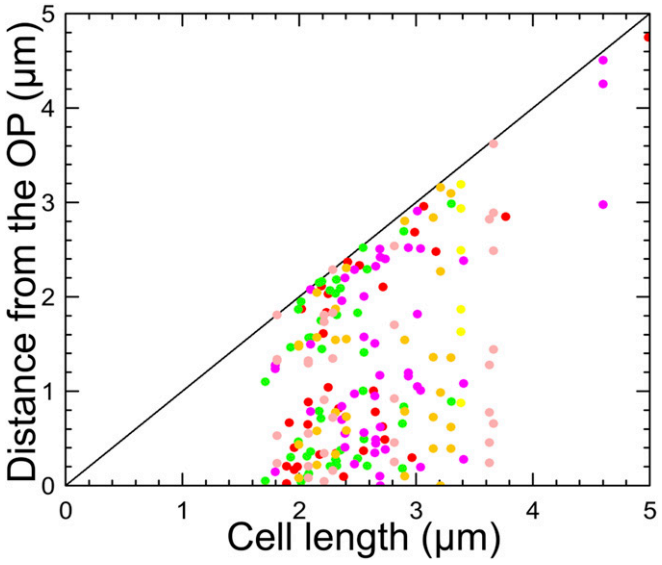


**Fig. 6.** Replication and segregation of the Ti plasmid. Distance of eGFP-RepB-Ti foci from the old pole in 100 cells containing one (red), two (green), three (magenta), four (orange), five (pink), or six (yellow) foci.

## Discussion

We investigate the patterns of replication and segregation of the four replicons of *Agrobacterium* during its polar growth cell cycle. Larger replicons replicate in a distinct temporal order: first, CC; second, pAt; and third, LC. Their replication is also spatially distinct: CC always replicates at the OP suggesting a factor(s) must mediate its localization. In contrast, while LC and pAt localize initially close to the OP, they migrate anywhere between the OP and the other end of the OP compartment prior to replication. That pTi can be everywhere in the old or new cell compartments prior to replication, and pTi undergoes one or two rounds of replication per cell cycle, suggests there is no active segregation mechanism. Below we discuss notable features of the replication/segregation of the essential CC and LC during polar growth to provide insight into mechanisms underlying their faithful propagation.

Polar growth is intrinsically asymmetric. Once new GPs are formed at the septum, cell elongation begins as buds to generate the new cell compartments in sibling cells. The old cell compartment does not change in dimension during polar growth, while the new cell compartment undergoes major increases in diameter and length until it reaches the size of the old cell compartment (20). Such asymmetries may underlie asynchronous timing of CC and LC replication in sibling cells; both CC and LC replicate in the older sibling before they replicate in the younger sibling. The GP and OP identity factors PopZ and PodJ also exhibit asymmetries in the timing of their localization (16, 19). PopZ is removed from the GP during its transition to an OP and reappears at the "new" GP created by septation in the new cell compartment sibling (16). In contrast, in the old cell compartment sibling, PopZ must be synthesized de novo and localized to the "new" GP resulting from septation (16). PodJ is at the OP during the early stages of the cell cycle, and then PodJ appears at the GP when PopZ leaves and is essential for the transition of the GP to an OP (18, 19).

In fact, pole identity is critical to both the temporal and spatial regulation of *Agrobacterium* chromosome dynamics during replication/segregation. OP identity is already established in the older sibling, and this may promote earlier replication of CC and LC; by contrast, the younger sibling must change the identity of its GP to an OP prior to division (Fig. 1); potentially, there is a maturation phase of this "new" OP to allow chromosome anchoring and subsequent replication. Here we present strong evidence for the role(s) of pole identity in chromosome replication/segregation: deletion of GP and OP identity factors, PopZ and PodJ, results in dramatically altered patterns of CC and LC replication/segregation. Without PopZ, cells lose their CC and LC, implicating PopZ in segregating and/or anchoring chromosomes to GPs post replication. Ehrle et al. (16) also observed loss of the CC in the absence of PopZ. Early in the cell cycle prior to replication, we demonstrate that correct localization of the CC and LC to the OP is mediated by PodJ.

The critical importance of PodJ in *Agrobacterium* chromosome dynamics is underscored by the following numerous abnormal phenotypes produced in the absence of PodJ. 1) The fate of the GP is not fixed; either it continues as a GP in the next cell cycle, or it does not, and this choice occurs with approximately equal frequency. When the GP is not used for continued growth in the next cell cycle, the CC migrates to the middle of the GP compartment prior to cell division and subsequent replication. 2) Replicated CCs do not localize to the OP at the end of the cell cycle, but instead either remain at the GP in the GP compartment, or localize in the middle of the NGP compartment. 3) As the CC can replicate at the GP or in the middle of the NGP compartment, it does not require factors at the OP for replication to occur. 4) The LC colocalizes with the CC and exhibits the above three abnormal phenotypes.

An understudied feature of polar growth is the generation of a presumptive division site, observed as a "constriction" between old and new cell compartments that develops soon after polar growth initiates. This constriction may restrict movement of replicons from the old to the new cell compartment. In contrast, during cell elongation by circumferential longitudinal growth, the growing cell has the same diameter along its length (22). In longitudinal growth in *Caulobacter*, a gradient of ParA ATPase drives movement of the replicated chromosome to one end of the cell, and the gradient shrinks in late stages of the cell cycle when segregation in complete (23, 24). By analogy, segregation of CC and LC may be facilitated by ParA and RepA gradients, respectively, that act sequentially. To date, all we know is that replication/segregation cassettes confer specificity (25); when the *repABC* system of *Sinorhizobium* megaplasmid pSymA was transferred to a small plasmid it exhibited the replication/segregation pattern of pSymA (26).

Besides PopZ, what factors might mediate GP localization of the CC and LC in *ΔPodJ* cells? At first glance, growth-pole-ring protein (GPR) might be an obvious candidate based on its precise three-dimensional structure at the GP (27) compared to the

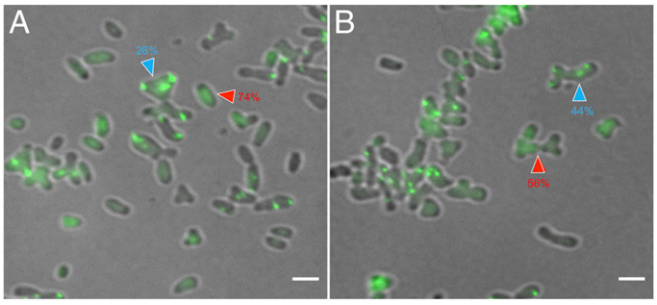


**Fig. 7.** Segregation of CC and LC is inefficient in PopZ-depleted cells. (*A*) Localization of eGFP-ParB in PopZ-depleted cells. Percentage of cells expressing eGFP-ParB showing diffuse fluorescence (red arrowhead) or multiple foci (blue arrowhead). (*B*) Localization of eGFP-RepB (LC) in PopZ-depleted cells. Percentage of cells expressing eGFP-RepB (LC) showing diffuse fluorescence (red arrowhead) or multiple foci (blue arrowhead). (Scale bars, 2 μm.)

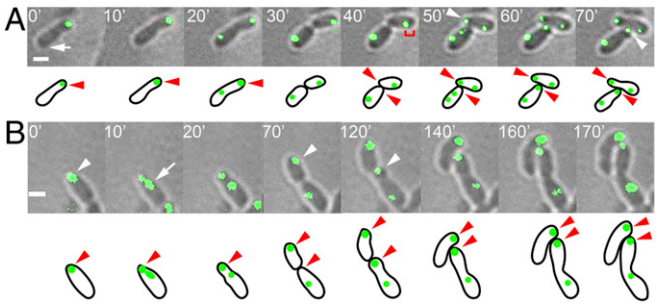


**Fig. 8.** CC localization is altered in Δ*podJ* cells. CCs were monitored by eGFP-ParB in time-lapse imaging. (*A*) Cell where GP transitions to an NGP. CC (in cell that did not transition in previous cycle) localizes to the GP and not the NGP (0′, white arrow). After replication (20′), one copy remains at GP, and one copy moves to the NGP compartment. As the GP transitions to an NGP, CC moves to the middle of the cell (40′, red bracket). Post division, CC replication occurs near the middle of both sibling cells (50′); one copy localizes to the GP (50′ and 70′, white arrowheads), while one copy remains in the NGP compartment in each sibling. (*B*) Cell where GP fails to transition to an NGP. Initially, the CC is at the GP (0′, white arrowhead). After CC replication at the GP (10′, white arrow); one copy remains at the GP (20′–170′), and one copy moves into the NGP compartment (20′). At septation, the GP in the upper cell does not become an NGP (70′, upper cell, white arrowhead), and growth continues from this pole (70′–170′). In the lower cell after replication, one copy of the CC localizes at the GP created at the septation site (120′, lower cell, white arrowhead), and one copy is in the NGP compartment cell. CC position is indicated by green circles, and GPs are indicated by red arrowheads in the accompanying diagrams. (Scale bar, 1 μm.)

intrinsically disordered structure of PopZ (28). However, GPR is present in cells lacking PopZ; yet, multiple growth poles and abnormal chromosome segregation still occur. Instead, GPR is more likely an organizing center for peptidoglycan and lipid biogenesis at the GP during polar growth (27).

In summary, PodJ is required, directly or indirectly, to localize the CC and LC at/near the OP prior to replication in new sibling cells, and post replication, PopZ is essential for GP localization of CC and LC. A fascinating unanswered question is what happens when the GP transitions into an OP? Are PopZ and PodJ sufficient, or are additional factors required to anchor chromosomes during the switch in pole identity? How does PodJ anchor the CC strongly to the tip of the OP and allow replication of the CC before it is released to migrate to the GP compartment? Are additional OP factors required? Whatever factors mediate OP localization, OP localization per se is not essential for CC or LC replication, as CC and LC can replicate when positioned at the GP or the middle of the NGP compartment in Δ*podJ*. What determines that LC and pAt are less tightly anchored to the OP tip as they migrate away from the tip prior to replication? Finally, what determines the order of replication/segregation of CC, pAt, and LC? Notably, in *Sinorhizobium*, primary chromosome partitioning genes are expressed 20′–30′ before pSym megaplasmid partitioning genes (29). Thus, timing of replicon segregation may be partly regulated by transcriptional regulation of partitioning proteins.

Future studies will provide novel insights into the evolution and function of *Agrobacterium*-specific PopZ/PodJ mediated replicon dynamics, especially given that what occurs in *Agrobacterium* (16–19, 21) is remarkably different from what is known in the best studied PopZ/PodJ system in *Caulobacter cresentus* (30–34). Segregation of the chromosome in *Caulobacter* is all about PopZ. PopZ anchors the chromosome at the old pole, and then PopZ accumulates at the new pole as replication starts. Finally, PopZ at the new pole tethers one copy of the chromosome so that each sibling inherits a chromosome. In further contrast, in *Caulobacter*, PodJ tethers the histidine kinase PleC at the new pole to regulate morphogenesis of the swarmer pole (34). The *Agrobacterium* PodJ is longer than *Caulobacter* PodJ (by 273 amino acids [aa]) and only shares 23% aa identity (19), so it may have evolved different function(s). Finally, the multipartite genome of *Agrobacterium* offers additional complexities to the list of unsolved mechanisms that coordinate their spatiotemporal replication and segregation during polar growth.

## Materials and Methods

**Plasmid Construction.** Standard molecular cloning techniques were used (35). We used GenBank AE007869.2, AE007870.2, AE007872.2, and AE007871.2 for nucleotide sequences of the CC, LC, pAt, and pTi, respectively. Genomic DNA was prepared from an exponential growth-phase culture of *A. tumefaciens* C58 using the Qiagen DNeasy Blood and Tissue kit according to the instructions for Gram-negative bacteria. Polymerase chain reaction (PCR) was performed with the proofreading enzyme Phusion HF DNA Polymerase and the High GC buffer (New England Biolabs). PCR conditions were determined empirically for each gene of interest. For pJZ254, the coding sequence for *parB* (Atu2828, GenBank AAK88539.2) was amplified by PCR from *Agrobacterium* genomic DNA with AvrII and HindIII sites at the 5′ and 3′ ends, respectively, and ligated into pJZ210 (27) using these restriction sites. For pACE001, the coding sequence for *repB* (Atu3923, GenBank AAK89497.1) was amplified by PCR from *Agrobacterium* genomic DNA with AvrII and HindIII sites at the 5′ and 3′ ends, respectively, and ligated into pRG019 (19) using these restriction sites. For pREJS001, *egfp* was cloned from pJZ253 (27) into pSRKKm (36) using NdeI and XbaI restriction sites. *repB* (Atu2828, GenBank AAK88539.2), *repB-At* (Atu5001, GenBank AAK9038.1), and *repB-Ti* (Atu6044, GenBank AAK91002.1) were amplified by PCR from *A. tumefaciens* strain C58 genomic DNA with XbaI and KpnI restriction sites at their 5′ and 3′ ends, respectively, and introduced into the single copy number plasmid pREJS001 (*SI Appendix*, Table S2) using these restriction sites to create pREJS002, pREJS003, and pREJS004, respectively. All constructs were verified by sequencing. *SI Appendix*, Table S2 contains additional information on plasmids and strains. Resulting plasmids, based on pSRK vectors (36), placed cloned genes under control of a tightly regulated lactose-

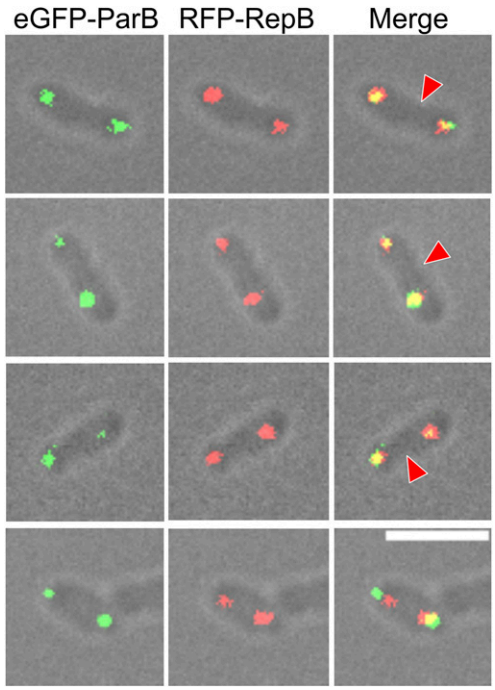


**Fig. 9.** LC mislocalization is similar to CC in Δ*podJ* cells. CC monitored by eGFP-ParB (*Left*) and LC monitored by eGFP-RepB-LC (*Middle*) in four cells. (*Right*) Merged images with yellow fluorescence indicating colocalization. Red triangles indicate (slight) constriction at base of the shorter GP compartment cell. The GP could not be identified in the bottom cell. CCs and LCs are colocalized (yellow fluorescence) or in close proximity in all cases (*Right*). From top to bottom, cells shown are numbers 30, 45, 54, and 25, respectively, seen in *SI Appendix*, Fig. S5. (Scale bar, 2 μm.)

inducible promoter resulting in expression between 10 and 20% of WT levels (15).

**Bacterial Strains and Growth Conditions.** Cloning of above plasmids was performed using *Escherichia coli* XL Blue. All *Agrobacterium* strains were grown in LB at 28 °C. When appropriate, growth media were supplemented with 50 μg/mL gentamicin and/or 40 μg/mL kanamycin to select for plasmids carrying GFP fusion constructs. The riboswitch-*popZ* strain (17) was grown with 0.5 mM theophylline to induce PopZ expression; for depletion experiments, cells were grown overnight in the absence of theophylline.

**Fluorescence and Time-Lapse Microscopy.** Lactose-inducible expression of cloned partitioning genes was achieved by diluting overnight cultures to $10^8$ cells/mL and adding 0.25 mM isopropyl β-D-1-thiogalactopyranoside for 3–4 h before single-time or time-lapse imaging as described (17). For widefield fluorescence, cells were imaged on LB 1% agarose pads. All images were processed using Fiji/ImageJ software (37). Cell length and position of the fluorescent foci were determined using ObjectJ (38). Each image was scaled to 15.5 px/μm. Time-lapse imaging was performed using the CellASIC ONIX system (EMD Millipore) as described (17).

**Data Availability.** All study data are included in the article and *SI Appendix*.

**ACKNOWLEDGMENTS.** We thank Steven Ruzin, Ph.D., and Denise Schichnes, Ph.D., at the College of Natural Resources Biological Imaging Facility at University of California, Berkeley, for assistance with fluorescent imaging. The Biological Imaging Facility is supported in part by National Institutes of Health Program S10 (Award 1S1OD018136-01). Research in the P.Z. laboratory is supported by National Science Foundation Grant MCB-0923840. J.S.R.-E. received fellowship support from the Secretaría Nacional de Educación Superior, Ciencia, Tecnología, e Innovación, Ecuador.

1. M. A. Cevallos, R. Cervantes-Rivera, R. M. Gutiérrez-Ríos, The repABC plasmid family. *Plasmid* **60**, 19–37 (2008).
2. U. M. Pinto, K. M. Pappas, S. C. Winans, The ABCs of plasmid replication and segregation. *Nat. Rev. Microbiol.* **10**, 755–765 (2012).
3. B. Goodner *et al*., Genome sequence of the plant pathogen and biotechnology agent *Agrobacterium tumefaciens* C58. *Science* **294**, 2323–2328 (2001).
4. D. W. Wood *et al*., The genome of the natural genetic engineer *Agrobacterium tumefaciens* C58. *Science* **294**, 2317–2323 (2001).
5. G. C. diCenzo, T. M. Finan, The divided bacterial genome: Structure, function, and evolution. *Microbiol. Mol. Biol. Rev.* **81**, 208 (2017).
6. F. Galibert *et al*., The composite genome of the legume symbiont *Sinorhizobium meliloti*. *Science* **293**, 668–672 (2001).
7. E. G. Ruby *et al*., Complete genome sequence of *Vibrio fischeri*: A symbiotic bacterium with pathogenic congeners. *Proc. Natl. Acad. Sci. U.S.A.* **102**, 3004–3009 (2005).
8. S. M. Halling *et al*., Completion of the genome sequence of *Brucella abortus* and comparison to the highly similar genomes of *Brucella melitensis* and *Brucella suis*. *J. Bacteriol.* **187**, 2715–2726 (2005).
9. J. F. Heidelberg *et al*., DNA sequence of both chromosomes of the cholera pathogen *Vibrio cholerae*. *Nature* **406**, 477–483 (2000).
10. T. G. Platt, E. R. Morton, I. S. Barton, J. D. Bever, C. Fuqua, Ecological dynamics and complex interactions of *Agrobacterium* megaplasmids. *Front. Plant Sci.* **5**, 635 (2014).
11. E. W. Nester, *Agrobacterium*: Nature's genetic engineer. *Front. Plant Sci.* **5**, 730 (2015).
12. L. S. Kahng, L. Shapiro, Polar localization of replicon origins in the multipartite genomes of *Agrobacterium tumefaciens* and *Sinorhizobium meliloti*. *J. Bacteriol.* **185**, 3384–3391 (2003).
13. P. J. B. Brown *et al*., Polar growth in the Alphaproteobacterial order Rhizobiales. *Proc. Natl. Acad. Sci. U.S.A.* **109**, 1697–1701 (2012).
14. E. Kuru *et al*., In situ probing of newly synthesized peptidoglycan in live bacteria with fluorescent D-amino acids. *Angew. Chem. Int. Ed. Engl.* **51**, 12519–12523 (2012).
15. J. R. Zupan, T. A. Cameron, J. Anderson-Furgeson, P. C. Zambryski, Dynamic FtsA and FtsZ localization and outer membrane alterations during polar growth and cell division in *Agrobacterium tumefaciens*. *Proc. Natl. Acad. Sci. U.S.A.* **110**, 9060–9065 (2013).
16. H. M. Ehrle *et al*., Polar organizing protein PopZ is required for chromosome segregation in *Agrobacterium tumefaciens*. *J. Bacteriol.* **199**, 752 (2017).
17. R. Grangeon, J. Zupan, Y. Jeon, P. C. Zambryski, Loss of $PopZ_{At}$ activity in *Agrobacterium tumefaciens* by deletion or depletion leads to multiple growth poles, minicells, and growth defects. *MBio* **8**, e01881-17 (2017).
18. J. C. Anderson-Furgeson, J. R. Zupan, R. Grangeon, P. C. Zambryski, Loss of PodJ in *Agrobacterium tumefaciens* leads to ectopic polar growth, branching, and reduced cell division. *J. Bacteriol.* **198**, 1883–1891 (2016).
19. R. Grangeon, J. R. Zupan, J. Anderson-Furgeson, P. C. Zambryski, PopZ identifies the new pole, and PodJ identifies the old pole during polar growth in *Agrobacterium tumefaciens*. *Proc. Natl. Acad. Sci. U.S.A.* **112**, 11666–11671 (2015).
20. T. A. Cameron, J. Anderson-Furgeson, J. R. Zupan, J. J. Zik, P. C. Zambryski, Peptidoglycan synthesis machinery in *Agrobacterium tumefaciens* during unipolar growth and cell division. *MBio* **5**, e01219-14 (2014).
21. M. Howell *et al*., Absence of the polar organizing protein PopZ causes aberrant cell division in *Agrobacterium tumefaciens*. *J. Bacteriol.* **199**, e00101-17 (2017).
22. N. Ouzounov *et al*., MreB orientation correlates with cell diameter in *Escherichia coli*. *Biophys. J.* **111**, 1035–1043 (2016).
23. W. B. Schofield, H. C. Lim, C. Jacobs-Wagner, Cell cycle coordination and regulation of bacterial chromosome segregation dynamics by polarly localized proteins. *EMBO J.* **29**, 3068–3081 (2010).
24. H. C. Lim *et al*., Evidence for a DNA-relay mechanism in ParABS-mediated chromosome segregation. *eLife* **3**, e02758 (2014).
25. P. Koper, K. Żebracki, M. Marczak, A. Skorupska, A. Mazur, RepB proteins of the multipartite *Rhizobium leguminosarum* bv. *trifolii* genome discriminate between centromere-like parS sequences for plasmid segregational stability. *Mol. Microbiol.* **102**, 446–466 (2016).
26. B. Frage *et al*., Spatiotemporal choreography of chromosome and megaplasmids in the *Sinorhizobium meliloti* cell cycle. *Mol. Microbiol.* **100**, 808–823 (2016).
27. J. R. Zupan, R. Grangeon, J. S. Robalino-Espinosa, N. Garnica, P. Zambryski, GROWTH POLE RING protein forms a 200-nm-diameter ring structure essential for polar growth and rod shape in *Agrobacterium tumefaciens*. *Proc. Natl. Acad. Sci. U.S.A.* **116**, 10962–10967 (2019).
28. J. A. Holmes *et al*., *Caulobacter* PopZ forms an intrinsically disordered hub in organizing bacterial cell poles. *Proc. Natl. Acad. Sci. U.S.A.* **113**, 12490–12495 (2016).
29. N. J. De Nisco, R. P. Abo, C. M. Wu, J. Penterman, G. C. Walker, Global analysis of cell cycle gene expression of the legume symbiont *Sinorhizobium meliloti*. *Proc. Natl. Acad. Sci. U.S.A.* **111**, 3217–3224 (2014).
30. G. R. Bowman *et al*., A polymeric protein anchors the chromosomal origin/ParB complex at a bacterial cell pole. *Cell* **134**, 945–955 (2008).
31. G. Ebersbach, A. Briegel, G. J. Jensen, C. Jacobs-Wagner, A self-associating protein critical for chromosome attachment, division, and polar organization in *Caulobacter*. *Cell* **134**, 956–968 (2008).
32. J. L. Ptacin *et al*., Bacterial scaffold directs pole-specific centromere segregation. *Proc. Natl. Acad. Sci. U.S.A.* **111**, E2046–E2055 (2014).
33. P. H. Viollier, N. Sternheim, L. Shapiro, Identification of a localization factor for the polar positioning of bacterial structural and regulatory proteins. *Proc. Natl. Acad. Sci. U.S.A.* **99**, 13831–13836 (2002).
34. A. J. Hinz, D. E. Larson, C. S. Smith, Y. V. Brun, The *Caulobacter crescentus* polar organelle development protein PodJ is differentially localized and is required for polar targeting of the PleC development regulator. *Mol. Microbiol.* **47**, 929–941 (2003).
35. MR Green, J Sambrook, *Molecular Cloning: A Laboratory Manual*, (Cold Spring Harbor Laboratory Press, ed. 4, 2012).
36. S. R. Khan, J. Gaines, R. M. Roop 2nd, S. K. Farrand, Broad-host-range expression vectors with tightly regulated promoters and their use to examine the influence of TraR and TraM expression on Ti plasmid quorum sensing. *Appl. Environ. Microbiol.* **74**, 5053–5062 (2008).
37. J. Schindelin *et al*., Fiji: An open-source platform for biological-image analysis. *Nat. Methods* **9**, 676–682 (2012).
38. N. O. E. Vischer *et al*., Cell age dependent concentration of Escherichia coli divisome proteins analyzed with ImageJ and ObjectJ. *Front Microbiol.* **6**, 586 (2015).